Systematic analysis of factors that improve HDR efficiency in CRISPR/Cas9 technique

Foschi Nicola[1], Athanasakis Emmanouil[2], Gasparini Paolo[1,2], Di Stazio Mariateresa[2]*†, d'Adamo Adamo Pio[1,2]†

[1] Department of Medicine, Surgery and Health Sciences, University of Trieste, Italy
[2] Institute for Maternal and Child Health-IRCCS "Burlo Garofolo", Trieste, Italy

†These authors jointly supervised this work: Di Stazio Mariateresa, d'Adamo Adamo Pio

*Corresponding author
distazio@gmail.com
phone number:+39 0403785539

Abstract

The bacterial CRISPR/Cas9 system has a proven to be an efficient tool for genetic manipulation in various organisms, but the efficiency of sequence replacement by homologous direct repair (HDR) is substantially lower than random creation of indels. Many studies focused on improving the efficiency of HDR using double sgRNA, cell synchronization cycle and the delivery of ssODN with a rational design.

In the present study, we tested and compared the combination of these three methods to improve HDR efficiency. To our tests, we chosen the *TNFα* gene (NM_000594) for its crucial role in a variety of biological processes and diseases.

Our results showed a dramatically increases of HDR efficiency from undetectable HDR event to 39% of HDR efficiency and provide a new strategy to facilitate CRISPR/Cas9-mediated human genome targeting.

Furthermore, we showed that *TNFα* gene could be edited with CRISPR/Cas9 methodology, an opportunity to safely correct, in the future, the specific mutations of each patient.

Introduction

In the last decade, the use of the novel CRISPR-associated endonuclease Cas9 protein has been implemented for analytical and therapeutic approaches, in a broad spectrum of cell types and model organisms (1)(2). After the introduction of this technique, the creation of a knock-in and knock-out gene has become as simple, rapid, and economical

as never before.

The CRISPR/Cas9 system takes advantage of the ability of the bacterial Cas9 nuclease to induces DNA double-strand breaks (DBS) in a trinucleotide region repeated in the genome (the proto-spacer adjacent motifs or PAM), directed by a 20–22 bp synthetic RNA sequence (gRNA) located next to PAM (1).

Then, DBS stimulates the cells repair mechanisms including non-homologous recombination end joining (NHEJ) and homologous direct recombination (HDR) to repair the DNA strands (3)(4)(5)(6)(7)(8)(9).

NHEJ creates insertions and deletions in the target DNA sequence, thus producing a frameshift that abolishes the correct protein production, while HDR-based targeting has been widely used to manipulate coding or non-coding regions of DNA by introducing selected DNA sequences in the correct context.

In the fast-evolving field of gene editing using CRISPR/Cas9 important efforts to improve the efficiency of the generation of targeted variants have been made; however, the reported success rates remain very low in many cells type and *in vivo* studies (10)(11)(5).

So far, many protocols have been published that describe how to improve the efficiency of HDR. Acosta et al. described a highly efficient HDR targeting approach based on the use of two sgRNAs flanking the targeted region, in mouse ESC lines in three different loci by a new method called “two gRNA-driven homozygous HR” (1). Zhou at al. reported that the use of dual sgRNAs increases the endogenous gene targeting efficiency in mouse cells (1,12).

Other authors tried to improve the HDR by blocking the cells cycle at different phases, showing that treatment with nocodazole, increases the efficiency of HDR. Nocodazole blocks cells at G2/M phase when DNA is completely replicated and the nuclear membrane is broken, allowing Cas9 to easily access DNA and enhancing the HDR (13).

Richardson et al. focused on understanding how Cas9 enzyme interacts, cuts and dissociates from the target DNA in physiological condition to improve the genome editing by HDR event. They showed that the enzyme locally releases the PAM-distal non-target strand after cleavage but before complete dissociation, making this strand available for complementary annealing of ssODN. For this reason, the ssODN with asymmetric arms with the arm of 36bp on the PAM-distal side and the 91bp arm on the PAM-proximal site of the break, complementary to non-target DNA strand, seems to have the highest efficiency of HDR (14).

These results inspired us to investigate the effect on HDR combining the three approaches described. We wondered if the three protocols synergically increase the efficiency of HDR.

For this aim, we have chosen the *TNFα* gene (NM_000594) for its crucial role in a variety of biological processes and diseases. *TNFα* encodes a multifunctional proinflammatory cytokine that belongs to the tumor necrosis factor superfamily. This cytokine is involved in the regulation of a wide spectrum of biological events, such as immune cell regulation, cell proliferation, differentiation, apoptosis, lipid metabolism, coagulation and thus is implicated in a variety of diseases (15)(16)(17). *TNFα* is also involved in rheumatoid arthritis (RA), a complex autoimmune disease, with a relatively constant prevalence of 0,5-1% in the world's populations that affect many organs; including kidney, eyes, spleen, heart, and lungs (18). In addition, *TNF*α can alters the regulation of insulin response, and its expression plays a role in the pathophysiology of insulin resistance (19). Recent studies focused their attention on the role of the proinflammatory cytokine tumor necrosis factor in the development of heart failure showing a direct relationship between the level of *TNFα* expression and the severity of heart disease (20). Furthermore, this cytokine has a relevance in tumor immune surveillance, and play crucial roles in tumor development and progression (15).

Based on this scenario, the possibility of modifying this gene became a fascinating and intriguing objective to safely correct, in the future, the specific mutations of each patient. Here we report a simple and robust approach to edit this gene.

Material and methods

Design of the sgRNAs and Plasmid Constructions

Two different sgRNAs were designed according to the following criteria: close location to the mutation(s); following PAM at the 3'end; and 20-nt length. The sgRNA were purchased by IDT (Integrated DNA Technologies, IDT, USA). The sgRNA consists of two RNA domains: crispr RNA (crRNA), which is specifically designed to be complementary to the target locus, and the constant trans-activating crRNA (tracrRNA), which is required for coupling with the Cas9 nuclease. The crRNAs were already cloned in pX333-U6-Chimeric_BB-CBh-hSpCas9 (Addgene, plasmid ID #42230). The two opposite BbsI and BsaI restriction sites were used to insert the guides under the control of a U6 promoter. For this purpose, self-complementary

103 oligonucleotides (Integrated DNA Technologies, IDT, USA) were annealed by gradual
104 cooling with prior denaturalization at 94° C. The duplex oligonucleotides also presented
105 cohesive ends with the 3' overhangs left after pX333 incubation with the BbsI and BsaI
106 restriction enzymes, serving for the ligation of the insert-plasmid with T4 DNA ligase
107 (EL0014; Thermo Fisher Scientific, Waltham, MA, USA). Moreover, the sgRNA1 and
108 sgRNA2 were cloned in the plasmid pX459 (Addgene, plasmid ID #62988), which
109 shows the puromycin antibiotic resistance. DH5α competent cells were transformed
110 with each of the plasmid constructs for Ampicillin selection and amplification in liquid
111 culture. The vectors were purified using a HiSpeed Plasmid Midi Kit (QIAGEN,
112 Hilden, Germany) and were Sanger sequenced to verify the correct cloning of the
113 specific crRNA inserts.
114
115 **HEK293 Cell Culture and Transfections**
116 HEK 293 cells were maintained in DMEM (Invitrogen) supplemented with 10% heat-
117 inactivated fetal bovine serum (FBS), 100 U/mL penicillin and 100 µg/mL
118 streptomycin at 37°C under 5% CO_2. $5x10^5$ cells were transfected with 3ug of plasmids
119 using Fugene transfection reagent (Promega). For the directed editing, 3ug of plasmid
120 was delivered to $5x10^5$ HEK293 cells with 1uL of the pertinent ssODN at 10 µM (10
121 pmol). The nocodazole was added after transfection at concentration of 100 ng/mL for
122 24 hours. Each Cas9-gRNA vector was co-transfected in HEK293 cells with an empty
123 CRISPR vector coding for a green fluorescent protein (pX458 Addgene, plasmid ID
124 #48138), in order to monitor the transfection efficiency. All experiments were assayed
125 in triplicate.
126
127 **PCR amplification of target region**
128 A 1286 nt region of *TNFα* locus, containing the target site, were PCR amplified using
129 the following primer sets. The target locus was amplified for 35 cycles with specific
130 forward (TNF-X-Fw:5'-CGCCACCACGCTCTTCTG-3') and reverse (TNF-Alw-
131 Rv:5'-CGGTCCAGCCACTGGAGC-3') primers targeting exon 1 and exon 4 of the
132 *TNF*α gene. The PCR reaction was performed using 200 ng of genomic DNA and Kapa
133 Hot start high-fidelity polymerase (Kapa Biosystems, Wilmington, MA) in high GC
134 buffer according to the manufacturer's protocol. The thermocycler setting consisted of

135 one cycle of 95°C for 5 min, 35 cycles of 98°C for 20 s, 61°C for 15 s and 72°C for 30
136 s, and one cycle of 72°C for 1 min. The PCR products were analyzed on 1,3% agarose
137 gel containing Midori Green Xtra (NIPPON Genetics Europe, Dueren, Germany). The
138 concentration of PCR DNA was quantitated based on the band intensity relative to a
139 DNA standard using the software Image Lab (Bio-Rad, Hercules, CA). About 200 ng
140 of PCR DNA was used for T7 endonuclease I and SmaI analyses.
141
142 **T7-Endonuclease I Assay**
143 The widely used T7-endonucelase I assay targets and digests hetero-duplexes formed
144 by hybridization of mutant WT strands resulting in two smaller fragments, and this
145 method was performed to assess sgRNA-specific activity. After transfection, cells were
146 incubated for 48 hr. The cells were then pelleted, and the lysis performed using QIAamp
147 DNA Mini Kit (Qiagen). The PCR products were denatured and then reannealed using
148 the following program: 95° C for 5 min, ramp down to 85°C at 2°C/s, and ramp down
149 to 25°C at 0.1 C/s. Immediately after the reannealing step, and the consequent
150 heteroduplex formation, 5 units of T7 endonuclease I (New England Biolabs, Ipswich,
151 MA) was added to the mix and incubated for 1 hr at 37°C. The product was resolved
152 on 1,3% agarose gel containing Midori Green Xtra (NIPPON Genetics Europe, Dueren,
153 Germany).
154
155 **Clonal Amplicon Sanger Sequencing**
156 A PCR product obtained from the target locus was cloned using a kit for sequencing
157 purposes (TOPO TA Cloning Kit, Thermo Fisher Scientific) and introduced in *E. coli*.
158 Sanger sequencing was used to sequence 10 individual colonies to reveal the clonal
159 genotype and thus the general indel and HDR frequency.
160
161 **Design of the ssODNs**
162 Single-stranded donor oligonucleotide (ssODN) for the HDR were designed with
163 symmetric (60nt long) and non-symmetric (90nt, 36nt long) homology arms, in both
164 orientation (5'-3';3'-5'), complementary to target and non-target DNA strand. The
165 ssODNs sequence includes a new and unique SmaI restriction site, juxtapose to the
166 homology arms. These ssODNs were synthesized as Ultramer Oligonucleotides
167 (Integrated DNA Technologies, IDT). Since the edited sequence contained a newly
168 acquired SmaI restriction site, PCR products of both amplifications were restricted

169 immediately after with SmaI enzyme (NEB, Ipswich, MA).
170
171 **Analysis of HDR by SmaI restriction digestion**
172 The reaction consisted of 1.6 µg of PCR DNA and 20 units of SmaI enzyme in CutSmart
173 Buffer (NEB, Ipswich, MA). After 1hr of incubation at 37°C, the reaction was arrested
174 with heat inactivation at 65°C for 20 min. The product was resolved on 1.3% agarose.
175 The band intensity was quantitated using Image Lab. The percentage of HDR was
176 calculated using the following equation (b + c / a + b + c) × 100 for the single cut
177 strategy, (b + c / a + b + c + d) x 100 for the dual cut strategy. In the first equation, 'a'
178 is the band intensity of DNA substrate and 'b' and 'c' are the cleavage products. In the
179 second equation, 'a' is the band intensity of DNA substrate wild type, 'b' and 'c' are
180 the cleavage products, and 'd' is the deleted fragment in which both sgRNA worked
181 properly but there wasn't a KI event. To further confirm the presence of the edited
182 sequence, conventional Sanger sequencing was performed **(Fig. S3A).**
183
184 **Off-target analysis**
185 To predict the most likely off-target sites for the sgRNAs used to knock-down the *TNFα*
186 gene in this study, we used a public webserver:
187 (https://eu.idtdna.com/site/order/designtool/index/CRISPR_PREDESIGN) able to
188 assess and prioritize potential CRISPR/Cas9 activity at off-target loci based on
189 predicted positional bias of a given mismatch in the sgRNA protospacer sequence and
190 the total number of mismatches to the intended target site. The CRISPR design tool
191 (IDT) scored a total of 202 (101 for sgRNA1 and 101 for sgRNA2) potential off-target
192 sites in the human genome. The off-targets are scored between 0 to 100, where a major
193 number indicate a lower possibility that the off-target occurs. The top three potential
194 off-target sites (11 ≤ score ≤ 26) for each sgRNA, and the first genomic locus
195 independently by its position on the off-target list, were assessed by T7 endonuclease
196 assay in HEK 293 cells.
197
198 **Results**
199 **Genome editing of the human *TNFα* gene**
200 With the aim of improving the efficiency of homologous direct recombination (HDR),
201 we tested and further combined three strategies already reported in literature able to
202 increase the HDR efficiency, but never used together. We wondered if these protocols

203 (use of double sgRNA, rational design of ssODNs and cells synchronization), could
204 work in synergy to improve the HDR efficiency. In parallel, we added a fourth
205 condition in which the cells were transfected three consecutive times.
206 For this aim we proceeded in two steps:
207 1) First, to increase the efficiency of excision of the Cas9 nuclease we explored and
208 compared the use of one sgRNA (who induces one DSB) and dual sgRNAs (who
209 induces two DSB) located in the region of *TNFα* gene.
210 2) Next, after choosing the best sgRNA strategy, we compared the use of various donor
211 ssODNs in synchronized and unsynchronized cells with single and multiple transfection
212 events.
213
214 **Selection of specific RNA guides for DSB induction**
215 For this purpose, we used the previously described *Staphylococcus pyogenes* nuclease,
216 that utilizes a human-codon optimized SpCas9 and a chimeric sgRNA expression
217 vector to direct efficient site-specific gene editing (21)(22). We designed two 20-nt long
218 sgRNA with a wide-spam of 473 nucleotide to guide Cas9 to introns 1 and 3 of the
219 *TNF*α gene (sgRNA1 and sgRNA2) **(Fig. 1).** Without the presence of donor DNA
220 containing the homology arms, cells repair the DNA primarily by NHEJ, leaving
221 insertion and/or deletion (indels). Considering the small introns size (≈300-600bp) in
222 *TNF*α locus, indels can involve adjacent exons and may generate frameshift mutations
223 that knocking-out the *TNFα* gene.
224 In detail, in pX333 plasmid the two sgRNAs were cloned as single guide (pX333-
225 sgRNA1; pX333-sgRNA2), in tandem combination (pX333-2sgRNA1/1; pX333-
226 2sgRNA2/2) and the two different guides were cloned in the same vector (pX333-
227 2sgRNA1/2). To asses if the plasmid with puromycin can helps for positive clone
228 selection, we cloned the two sgRNAs also in pX459 vector (pX459-sgRNA1 and
229 pX459-sgRNA2), a plasmid that carry the puromycin resistance. The seven constructs
230 thus obtained were further transfected into HEK293 cells and the puromycin antibiotic
231 was added for 48h only in cells transfected with pX459 vector.
232 To evaluate the efficiency of DNA cutting and NHJE repair after the use of sgRNA
233 guides, the genomic DNA was isolated from HEK293 cells and screened for the
234 presence of site-specific gene modification by PCR amplification and T7E1
235 endonuclease assay, of region around the target sites **(Fig.2A).**

236 The results showed detectable bands in pX333-sgRNA2, pX333-sgRNA2/2, pX459-
237 sgRNA2. The use of sgRNAs cloned in single or in tandem when co-expressed with
238 the SpCas9 nuclease was able to mediate gene modification with comparable level of
239 efficiency. No differences were finally detected between pX333 or pX459 plasmids
240 after puromycin selection, maybe due to high efficiency of transfection obtained in
241 HEK293 cells. Notably, HEK293 cells transfected with the 2sgRNA plasmid
242 (2sgRNA1/2) and not treated with T7E1 nuclease resulted in a full-length (FL) and in
243 short-edited (SE) amplicons confirming the expected deletion of the region between the
244 two selected protospacers **(Fig. 2A)**.
245 Moreover, the frequency of Indels in the cells transfected with all sgRNAs, were
246 measured by sequencing 10 PCR amplicons encompassing the target sites. As reported
247 in the figure 2B, the highest editing frequencies achieved were 50% and 75% using
248 sgRNA2 and 2sgRNA1/2 guides, respectively **(Fig. 2B)**. The types of insertions and
249 deletions at this locus presented variable patterns of rearrangements of the coding
250 sequence, insertion from 1 to 10 nucleotides and deletion from 5 to 930 nucleotides.
251 Deletion of region between the 2 PAMs was observed in the cells transfected with
252 2sgRNA plasmid (2sgRNA1/2) (~480nts).
253 Furthermore, we observed the predominance of a precise junction between the two
254 DSBs when 2sgRNA1/2 was transfected, a mechanism already described (1)(12)(23).
255 These data further confirmed that the dual sgRNA (2sgRNA) is the most efficient
256 method for DNA excision in the endogenous locus. Based on these genomic results, we
257 selected the sgRNA2 and the 2sgRNA1/2 guides for the following HDR editing.
258
259 **Homologous direct recombination efficiency (HDR)**
260 With the aim to improve the HDR efficiency we chose the plasmids pX333-sgRNA2
261 and the pX333-2sgRNA1/2 that showed a highest degree of DSB in HEK293
262 transfection. Traditional HDR gene editing requires long homology arms to allows
263 proper and high-specificity recombination. The use of Cas9-gRNAs directed
264 recombination allows the use of much smaller homology arms (~90 bp to 700 bp) with
265 higher recombination rates than conventional HDR (1).
266 We decided to assess the efficiency of HDR by transfection of single (pX333-
267 sgRNA2) and double sgRNA (pX333-2sgRNA1/2) coupled with a rational design of
268 ssODNs. The structure of ssODNs with asymmetric arms complementary to a non-
269 target locus with long arm on the PAM-proximal side and short arm on the PAM-distal

270 side of the break, has been previously reported to induce highest HDR efficiency (14).
271 However, we decided to test this asymmetric donor for the *TNFα* locus by comparing
272 it with other possible ssODN structures on HDR efficiency.
273 Thus, we generated twelve ssODN molecules having different sequences overlap
274 on the 5' and 3' side of the break, specific for pX333-sgRNA2 and pX333-2sgRNA1/2
275 guides, and complementary to either target or non-target DNA strand **(Fig.3A,5A)**. We
276 co-delivered these ssODNs in combination with single sgRNA and for the first time
277 with a couple sgRNAs (2sgRNA1/2).
278 To facilitate the selection of HDR events, we inserted a restriction site for the enzyme
279 SmaI in all the ssODNs. The pX333-sgRNA2 and pX333-2sgRNA1/2 plasmids and the
280 respectively six ssODNs were then co-transfected in HEK293 cells. In addition, we
281 introduced a nocodazole cells synchronization, described to improve the HDR (5).
282 Then, we included a fourth condition in which the cells were transfected three
283 consecutive times with the same donor and plasmid.
284 Since the edited sequences contain a newly acquired SmaI restriction site, the HDR
285 efficiency, can be easily detected using the digestion on PCR products obtained with
286 primers flanking the targeted locus.
287
288 **Single cut and HDR efficiency**
289 First, we determined the HDR efficiency with the co-delivery of pX333-sgRNA2 guide
290 (who induces single DSB) and six ssODN molecules (A-F). We compared the HDR
291 efficiency after SmaI digestion in single transfection events, triple transfection and with
292 nocodazole cells treatment. Notably, among the six ssODNs, only the donors A, C and
293 E showed HDR event **(Fig.3B,C,D,E).** The tree donors are all complementary to the
294 non-target DNA strand, and this observation is consistent with previous studies (14).
295 The donors A and C are able to induce HDR but only after nocodazole treatment though
296 with a low frequency of 5,4% and 3,9%, respectively. With triple transfections in
297 unsynchronized cells, donor A increase the HDR efficiency from not detectable to
298 10,5%, and donor C form non detectable to 9,3%. Donor E, after triple transfection,
299 increases the HDR efficiency of 1,4-fold. The highest HDR frequency achieved was
300 22.1% for donor E, with triple transfection and nocodazole cells treatment.
301 The graphic in **Fig. S1A,B** (supplementary figure) compares the HDR efficiency in
302 synchronized and unsynchronized cells in one and triple cell transfections, respectively.
303 The graphic in **Fig. S1C,D** instead, compares the HDR efficiency between single and

304 triple transfection in synchronized and unsynchronized cells. These data showed that
305 no significant differences have been detectable with nocodazole treatment in our
306 experimental condition, while the triple transfection increases the HDR efficiency, but
307 only for the ssODNs A, C and E. While the other three donors (B, D, F) characterized
308 to be complementary to target DNA strand didn't induce HDR event.
309 Notably, the donor E induces the highest HDR efficiency. It showed the same
310 structure described by Richardson et al. to be the best for the HDR, with asymmetric
311 arms complementary to a non-target locus with 90bp on the PAM-proximal side and
312 36bp extension arm on the PAM-distal side of the break (14). The HDR efficiency using
313 donor E increased up to 22%, (more than two-fold) with triple transfection in
314 synchronized cells **(Fig.4).**
315
316 **Dual cut and DBS efficiency**
317 Furthermore, we tested the HDR efficiency combining the use of dual 2sgRNA and
318 rational design of ssODNs. HEK293 cells have been co-transfected with px333-
319 2gRNA1/2 guide (who induces double DSB) and six ssODNs (G-N) **(Fig.5A).** Next,
320 we determined systematically the effect on HDR efficiency in controls, in nocodazole
321 synchronized cells and triple transfection.
322 To note, as already here described, a simple PCR amplification before the T7E1 assay,
323 (that shows the DNA deletions caused from 2sgRNA1/2) is sufficient to assess the DSB
324 efficiency in various experimental conditions. Interestingly, the DSB efficiency
325 increases more than three-fold with triple transfection in synchronized cells **(Fig.6A)**
326
327 **Dual cut and HDR efficiency**
328 We further compared the HDR efficiency using px333sgRNA1/2 and the six ssODNs
329 (G-N) with SmaI digestion **(Fig.5A)**. With the use of 2sgRNA1/2 all ssODNs designed
330 showed detectable SmaI digestion bands who indicates that HDR occurred in all
331 experimental condition used. The graphic in **Fig.S2** (supplementary figure) showed the
332 effect of nocodazole and triple transfection on HDR efficiency using double sgRNA
333 guides. Again, the nocodazole doesn't have a significant effect on HDR; while the triple
334 transfection increased the HDR for all donors of about 1,3-2,6 fold**.** The nocodazole
335 diminished the HDR efficiency except for donor M. The donor ssODN M, has the same
336 design of donor E (the most efficient donor in the single cut comparison) with a PAM
337 of 90bp proximal arm and a 36bp arm with a distal PAM complementary to a non-

338 target DNA strand, and it is the most efficient ssODN, achieving a HDR efficiency up
339 to 39% **(Fig.5B,C,D,E)**. The graphic in figure 6B compares the HDR efficiency of
340 donor M in all experimental conditions used. The HDR after triple transfection in sync
341 cells, increases up to 1,8-fold. As already reported in literature, even in *TNFα* locus, the
342 use of 2sgRNA dramatically increase the HDR compared to single sgRNA more than
343 double (1).
344 Collectively, the results demonstrated that the combination of 2sgRNA, asymmetric
345 donor and triple transfection, induce a dramatic increase of HDR, from undetectable to
346 39% HDR efficiency.
347
348 **Off-targets analyses**
349 To predict the most likely off-target sites for the sgRNAs used to edit the *TNFα* gene
350 in this study, we used a public webserver:
351 (https://eu.idtdna.com/site/order/designtool/index/CRISPR_PREDESIGN) able to
352 assess and prioritize potential CRISPR/Cas9 activity at off-target loci. The top three
353 potential off-target sites for each sgRNA were assessed by the T7E1 assay. None of the
354 loci analyzed showed detectable levels of off-target events **(Fig.S3B)**.
355
356 **Discussion**
357 Here, we report a new and simple approach to enhancer genome engineering in human
358 cells. We compared the use of single sgRNA with coupled 2sgRNA to edit the *TNFα*
359 locus. According to data already reported, our results showed that the use of 2sgRNA
360 increases dramatically the DSB efficiency. Furthermore, the use of 2sgRNA creates a
361 precise DNA excision between each PAM sequence, a huge advantage over the
362 randomly sized indels created by single sgRNA transfection **(Fig.2).** In addition, the
363 deletions between the 2sgRNA can be easily identified by PCR amplification and
364 agarose electrophoresis, thus avoiding the T7E1 assay. Further, the results showed that
365 the DSB increases after triple transfection up to two-fold and, in combination with
366 nocodazole treatment increases up to three-fold **(Fig.6).**
367 As already known, even in *TNF*α locus, the use of 2sgRNA increases the HDR
368 efficiency more than double compared to transfection of single sgRNA. This could be
369 explained by the capability of double 2sgRNA to create a precise cut on the target site,
370 oscillating from time to time only for a few bases, without generating unpredictable
371 indels. Otherwise, a single-cut approach, induces truly extensive deletions reducing a

372 lot the possibility of binding the arms of homology, thus leading to a drastic drop in
373 HDR rates.
374 We then tested the HDR frequency by transfecting various ssODN molecules with
375 different structure in combination with single sgRNA and 2sgRNA pair. In particular,
376 with the use of single sgRNA, we observed that donor DNA complementary to the non-
377 target strand are more effective than the ones complementary to target strand, and this
378 is consistent with previous studies performed with various ssODNs structure in human
379 cells (14), or using symmetric ssODNs to introduce mutations at the EMX1 and AAVS1
380 loci in human cell lines (5)(24) **(Fig.3)**. With the 2sgRNA pair since all ssODNs have
381 higher HDR efficiency, this effect is less marked **(Fig.5)**.
382 Our results further showed, again consistent with Richardson at al., that the
383 asymmetric ssODN donor complementary to non-target strand with the arm of 36bp on
384 the PAM-distal side and the 90bp arm on the PAM-proximal site of the break showed
385 the highest HDR efficiency using single sgRNA as well the couple 2sgRNA (donor E,
386 M) (14). The asymmetric donor allows the shorter arm to bind to distal PAM early
387 released strand, and the longer arm to bind to the PAM proximal portion of non-target
388 strand, by strand intrusion and complementary strand displacement. This donor
389 structure increases the HDR of about two-fold.
390 In contrast with literature data, we showed that the treatment with nocodazole doesn't
391 increase the HDR efficiency (13). Lin et al. showed a systematically studies of
392 nocodazole concentration on HDR efficiency. They transfected the cells after 17h of
393 the nocodazole treatment at concentration of 200ng/ml. They showed that the
394 nocodazole increases the HDR efficiency when is used in combination with low
395 concentration of Cas9 (30pmol), while 100pmol diminished the enhancement. Is
396 plausible to think that in our experimental condition, since we transfected a plasmid
397 who induces Cas9 expression to high dosage, we didn't use the correct Cas9
398 concentration to induces an increase in HDR efficiency. Moreover, we used 100ng/ml
399 of nocodazole that was added four hours after the transfection. In our experiments, the
400 nocodazole effect was detected only on the donor E and M, the best donor structures,
401 also capable of increasing HDR efficiency in cells synchronized with a wrong Cas9
402 concentration.
403 Interestingly the triple transfection increases the HDR from 1,3-2,6 fold. The triple
404 transfection was assessed in order to enrich the HDR cells colony expansion. Starting
405 by the evidence that any ssODNs, when properly integrated, destroy the sgRNA

recognition sequence; it has been decided to give a day of rest after every transfection event, in order to facilitate the HDR colony expansion. Due to the impossibility of re-modifying HDR colonies, the Cas9 protein is able to modify only non-recombinant cells.

In conclusion, our results showed that the highest HDR efficiency has been achieved when 2sgRNA, asymmetric donor (M) and triple transfection in synchronized cells were used. Using this system, we have maximized the efficiency of HDR, from undetectable HDR events (single guide, symmetric donor, unsynchronized cells, with single transfection) near to 40% HDR efficiency. We also proved that the *TNFα* gene can be edited with CRISPR/Cas9 methodology with high efficiency.

Finally, the results of our work can be used as a guideline to improve the efficiency (and the utility) of CRISPR/Cas9-mediated genome engineering using the most effective optimizations to date.

Author contributions

M.D.S., N.F. and A.P.D. conceived and designed the project. N.F. and M.D.S. performed the experiments. E.A. performed graphic analysis. M.D.S., A.P.D. and P.G. wrote the manuscript.

Conflict of interest statement

The authors declare that they have no conflict of interest.

Conflict of Interest

There are not conflict of interest to declare

References

1. Acosta S, Fiore L, Carota IA, Oliver G. Use of two gRNAs for CRISPR/Cas9 improves bi-allelic homologous recombination efficiency in mouse embryonic stem cells. Genesis [Internet]. 2018 May [cited 2018 Oct 24];56(5):e23212. Available from: http://doi.wiley.com/10.1002/dvg.23212
2. Fuster-García C, García-García G, González-Romero E, Jaijo T, Sequedo MD, Ayuso C, et al. USH2A Gene Editing Using the CRISPR System. Mol Ther Nucleic Acids [Internet]. 2017 Sep 15 [cited 2018 Oct 24];8:529–41. Available

440 from: https://linkinghub.elsevier.com/retrieve/pii/S2162253117302299
441 3. Latella MC, Di Salvo MT, Cocchiarella F, Benati D, Grisendi G, Comitato A,
442 et al. In vivo Editing of the Human Mutant Rhodopsin Gene by Electroporation
443 of Plasmid-based CRISPR/Cas9 in the Mouse Retina. Mol Ther Nucleic Acids
444 [Internet]. 2016 Nov 22 [cited 2018 Oct 24];5(11):e389. Available from:
445 http://www.ncbi.nlm.nih.gov/pubmed/27874856
446 4. Cong L, Ran FA, Cox D, Lin S, Barretto R, Habib N, et al. Multiplex genome
447 engineering using CRISPR/Cas systems. Science [Internet]. 2013 Feb 15 [cited
448 2018 Oct 25];339(6121):819–23. Available from:
449 http://www.sciencemag.org/cgi/doi/10.1126/science.1231143
450 5. Lin S, Staahl BT, Alla RK, Doudna JA. Enhanced homology-directed human
451 genome engineering by controlled timing of CRISPR/Cas9 delivery. Elife
452 [Internet]. 2014 Dec 15 [cited 2018 Oct 26];3. Available from:
453 https://elifesciences.org/articles/04766
454 6. Mali P, Yang L, Esvelt KM, Aach J, Guell M, DiCarlo JE, et al. RNA-guided
455 human genome engineering via Cas9. Science [Internet]. 2013 Feb 15 [cited
456 2018 Oct 25];339(6121):823–6. Available from:
457 http://www.sciencemag.org/cgi/doi/10.1126/science.1232033
458 7. Chandrasekaran AP, Song M, Kim K-S, Ramakrishna S. Different Methods of
459 Delivering CRISPR/Cas9 Into Cells. In 2018 [cited 2018 Oct 24]. p. 157–76.
460 Available from:
461 https://linkinghub.elsevier.com/retrieve/pii/S1877117318300796
462 8. Ran FA, Hsu PD, Wright J, Agarwala V, Scott DA, Zhang F. Genome
463 engineering using the CRISPR-Cas9 system. Nat Protoc [Internet]. 2013 Nov
464 24 [cited 2018 Oct 25];8(11):2281–308. Available from:
465 http://www.ncbi.nlm.nih.gov/pubmed/24157548
466 9. Mali P, Esvelt KM, Church GM. Cas9 as a versatile tool for engineering
467 biology. Nat Methods [Internet]. 2013 Oct [cited 2018 Nov 16];10(10):957–63.
468 Available from: http://www.ncbi.nlm.nih.gov/pubmed/24076990
469 10. Paquet D, Kwart D, Chen A, Sproul A, Jacob S, Teo S, et al. Efficient
470 introduction of specific homozygous and heterozygous mutations using
471 CRISPR/Cas9. Nature [Internet]. 2016 May 27 [cited 2018 Nov
472 16];533(7601):125–9. Available from:
473 http://www.ncbi.nlm.nih.gov/pubmed/27120160

474 11. Takayama K, Igai K, Hagihara Y, Hashimoto R, Hanawa M, Sakuma T, et al.
475 Highly efficient biallelic genome editing of human ES/iPS cells using a
476 CRISPR/Cas9 or TALEN system. Nucleic Acids Res [Internet]. 2017 May 19
477 [cited 2018 Nov 16];45(9):5198–207. Available from:
478 http://www.ncbi.nlm.nih.gov/pubmed/28334759
479 12. Zhou J, Wang J, Shen B, Chen L, Su Y, Yang J, et al. Dual sgRNAs facilitate
480 CRISPR/Cas9-mediated mouse genome targeting. FEBS J [Internet]. 2014 Apr
481 [cited 2019 Jun 12];281(7):1717–25. Available from:
482 http://doi.wiley.com/10.1111/febs.12735
483 13. Lin S, Staahl BT, Alla RK, Doudna JA. Enhanced homology-directed human
484 genome engineering by controlled timing of CRISPR/Cas9 delivery. Elife
485 [Internet]. 2014 Dec 15 [cited 2018 Oct 26];3:e04766. Available from:
486 http://www.ncbi.nlm.nih.gov/pubmed/25497837
487 14. Richardson CD, Ray GJ, DeWitt MA, Curie GL, Corn JE. Enhancing
488 homology-directed genome editing by catalytically active and inactive
489 CRISPR-Cas9 using asymmetric donor DNA. Nat Biotechnol [Internet]. 2016
490 Mar 20 [cited 2018 Oct 25];34(3):339–44. Available from:
491 http://www.nature.com/articles/nbt.3481
492 15. Yuepeng J, Zhao X, Zhao Y, Li L. Gene polymorphism associated with TNF-α
493 (G308A) IL-6 (C174G) and susceptibility to coronary atherosclerotic heart
494 disease. Medicine (Baltimore) [Internet]. 2019 Jan [cited 2019 May
495 15];98(2):e13813. Available from:
496 http://www.ncbi.nlm.nih.gov/pubmed/30633155
497 16. Dinarello CA. Anti-inflammatory Agents: Present and Future. Cell [Internet].
498 2010 Mar 19 [cited 2018 Nov 16];140(6):935–50. Available from:
499 http://linkinghub.elsevier.com/retrieve/pii/S0092867410002369
500 17. El-Tahan RR, Ghoneim AM, El-Mashad N. TNF-α gene polymorphisms and
501 expression. 2016 [cited 2019 Jun 3]; Available from:
502 https://www.ncbi.nlm.nih.gov/pmc/articles/PMC5014780/pdf/40064_2016_Art
503 icle_3197.pdf
504 18. Tumor Necrosis Factor - an overview (pdf) | ScienceDirect Topics [Internet].
505 [cited 2019 Jun 6]. Available from:
506 https://www.sciencedirect.com/topics/medicine-and-dentistry/tumor-necrosis-
507 factor/pdf

508 19. Malak CAA, Shaker OG, Ashour E, Magdy L. Genetic variations of the TNF-
509 α-308 G>A promoter, and TGF-β1 T869C polymorphisms in Egyptian
510 patients with rheumatoid arthritis [Internet]. Vol. 9, Int J Clin Exp Pathol. 2016
511 [cited 2019 May 23]. Available from: www.ijcep.com/
512 20. Ruan H, Hacohen N, Golub TR, Parijs L Van, Lodish HF. Tumor Necrosis
513 Factor-α Suppresses Adipocyte-Specific Genes and Activates Expression of
514 Preadipocyte Genes in 3T3-L1 Adipocytes. Diabetes [Internet]. 2002 May 1
515 [cited 2019 May 23];51(5):1319–36. Available from:
516 http://diabetes.diabetesjournals.org/content/51/5/1319
517 21. Zhang X, Wang J, Shao H, Zhu W. Function of tumor necrosis factor alpha
518 before and after mutation in gastric cancer. Saudi J Biol Sci [Internet]. 2017
519 Dec [cited 2019 May 23];24(8):1920–4. Available from:
520 https://linkinghub.elsevier.com/retrieve/pii/S1319562X17303145
521 22. Mali P, Yang L, Esvelt KM, Aach J, Guell M, DiCarlo JE, et al. RNA-Guided
522 Human Genome Engineering via Cas9. Science (80-) [Internet]. 2013 Feb 15
523 [cited 2018 Oct 25];339(6121):823–6. Available from:
524 http://www.sciencemag.org/cgi/doi/10.1126/science.1232033
525 23. Chen X, Xu F, Zhu C, Ji J, Zhou X, Feng X, et al. Dual sgRNA-directed gene
526 knockout using CRISPR/Cas9 technology in Caenorhabditis elegans. Sci Rep
527 [Internet]. 2014 Dec 22 [cited 2019 Aug 7];4:7581. Available from:
528 http://www.ncbi.nlm.nih.gov/pubmed/25531445
529 24. Yang L, Guell M, Byrne S, Yang JL, De Los Angeles A, Mali P, et al.
530 Optimization of scarless human stem cell genome editing. Nucleic Acids Res
531 [Internet]. 2013 Oct 1 [cited 2018 Oct 26];41(19):9049–61. Available from:
532 https://academic.oup.com/nar/article/41/19/9049/1189167
533
534
535 **Figure legends**
536
537 **Fig.1 CRISPR/Cas9 targeting of the human *TNF*α gene.** Schematic rapresentation
538 of human *TNF*α gene. The magnified view illustrates the sgRNAs (in red) and the
539 PAM sequences (in green).
540
541 **Fig.2 NHEJ-mediated knock-out of human *TNF*α gene using the CRISPR/Cas9**

542 **system. (A)** The T7EI nuclease assay on *TNFα* gene showed targeted cleavage of the
543 digested PCR products in HEK293 cells transfected with pX333-sgRNA1, pX333-
544 sgRNA1/1, pX459-sgRNA1, pX333-sgRNA 2, pX459-sgRNA2, pX333-sgRNA2/2
545 and pX333-sgRNA1/2 . Cells transfected with 2sgRNA shows the short edited PCR
546 product. (not determined, ND; negative control, NC; full-length, FL; short-edited,
547 SE). **(B)** Sequence analysis of PCR products surrounding the Cas9 target sites in the
548 genome of HEK293 transfected with sgRNA1, pX333-sgRNA1/1, pX333-sgRNA2,
549 pX333-sgRNA2/2 and pX333-2sgRNA1/2, (in bold) showed a wide variety of Indel
550 mutations mediated by NHEJ. The top sequence in red is the unmodified sequence, in
551 green are the PAMs. The mismatches/insertions are indicated in gray. The number of
552 PCR amplicons for each sequence is indicated in parentheses and the modified length
553 is indicated.
554
555 **Fig.3 Systematic investigation of DNA templates for efficient HDR at the *TNFα***
556 **locus in HEK293T cells. (A)** Segment of human *TNFα* shows the genome structure,
557 the sgRNA2 guide site and the primer used for PCR amplification (in violet). +1:
558 ATG. Six HDR templates (color coded) were tested for HDR efficiency, the PAM
559 region (in green). Template ssODN contains SmaI restriction sites (in red) that are
560 flanked by various lengths of homology arms. **(B)** HDR efficiency was tested in
561 single and triple transfection, in combination with synchronized cells. The mean %
562 HDR and standard deviation (error bar) was determined by SmaI digestion from three
563 experiments. Representative gels from PCR and HDR analyses are shown for each
564 cell condition.
565
566 **Fig.4 Graphic comparison of HDR efficiency of donor E.** The triple transfection
567 and nocodazole treatment increase the HDR efficiency of about two-fold. StUns,
568 Single transfection in unsynchronized cells; StSyn, Single transfection in
569 synchronized cells; TtUns, triple transfection in unsynchronized cells; TtSyn, triple
570 transfection in synchronized cells.
571
572 **Fig.5 Systematic investigation of DNA templates, and two sgRNA, for efficient**
573 **HDR at the *TNFα* locus in HEK293T cells.** (**A**) Segment of human *TNFα* shows
574 the genome structure, the two sgRNA 2 guides (sgRNA1, sgRNA2) sites and the
575 primer used for PCR amplification (in violet). +1: ATG

576 Six HDR templates (color coded) were tested for HDR efficiency, the PAM region (in
577 green). Template ssODNs contains SmaI restriction sites (in red) that are flanked by
578 various lengths of homology arms. (**B**) HDR efficiency was tested in single and triple
579 transfection, in combination with synchronized cells. The mean % HDR and standard
580 deviation (error bar) was determined by SmaI digestion from three experiments.
581 Representative gels from PCR and HDR analyses are shown for each cell condition.
582
583 **Fig.6 DSB efficiency with double sgRNA guides. (A)** Editing efficiency tested on
584 four different conditions. StUns= Single transfection unsynchronized, StSyn= Single
585 transfection nocodazole synchronization. **(B)** Single cut strategy and donor M, in
586 single and triple transfection, in synchronized and unsynchronized cells. The triple
587 transfection increase the HDR efficiency. StUns= Single transfection method,
588 unsynchronized cells; StSyn= Single transfection in synchronized cells, TtUns=
589 Triple transfection method in unsynchronized cells, TtSyn Triple transfection in
590 synchronized cells.
591
592 **Suppl. Fig.S1 Single cut stragtegy with sgRNA2 guide**. **(A, B)** HDR efficiency
593 between syncronized and non-syncronyzed cells, in single and triple transfection,
594 respectively. **C,D** HDR efficiency between single and triple transfection in
595 syncronyzed and unsyncronized cells.
596
597 **Suppl. Fig.S2 Double cut strategy with 2sgRNA1/2 guide**. **(A, B)** HDR efficiency
598 between syncronized and non-syncronyzed cells in single and triple transfection,
599 respectively. **C,D** HDR efficiency between single and triple transfection in
600 syncronyzed and unsyncronized cells.
601
602 **Suppl. Fig.S3**. **(A)** Sanger Sequence who showed the correct HDR events. **(B)**
603 Evaluation of CRISPR/Cas9 off-target effects for sgRNAs designed to knock-out the
604 human *TNFα* gene. T7 assay analysis at the top three potential off-target sites and the
605 first potential genic off-target site in HEK293T cells. OT: off-target locus
606
607

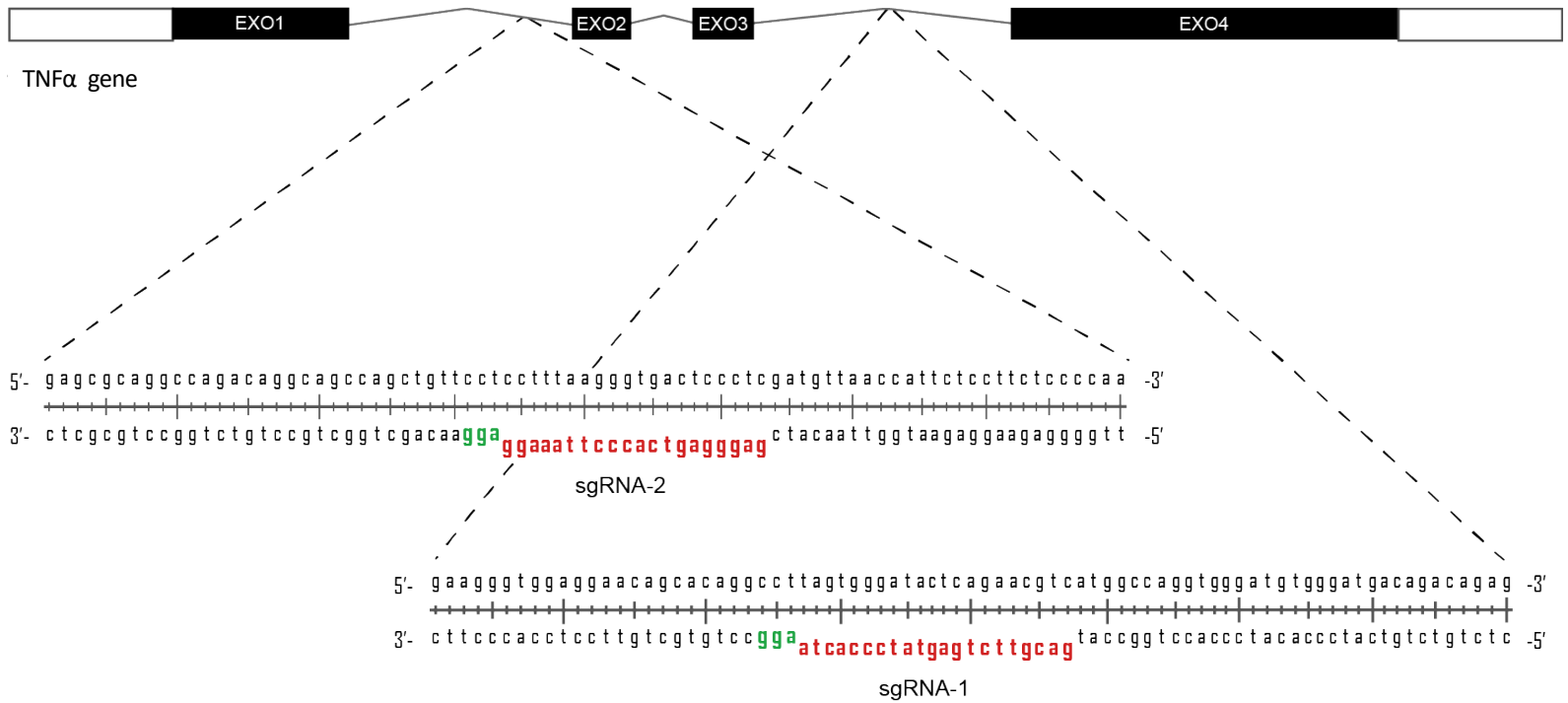
EXO1
EXO2
EXO3
EXO4
TNFα gene
5'- gagcgcaggccagacaggcagccagctgttcctcctttaagggtgactccctcgatgttaaccattctccttctccccaa -3'
3'- ctcgcgtccggtctgtccgtcggtcgacaaggaggaaattcccactgagggagctacaattggtaagaggaagaggggtt -5'
sgRNA-2
5'- gaagggtggaggaacagcacaggccttagtgggatactcagaacgtcatggccaggtgggatgtgggatgacagacagag -3'
3'- cttcccacctccttgtcgtgtccggaatcaccctatgagtcttgcagtaccggtccaccctacaccctactgtctgtctc -5'
sgRNA-1

Fig.1

A

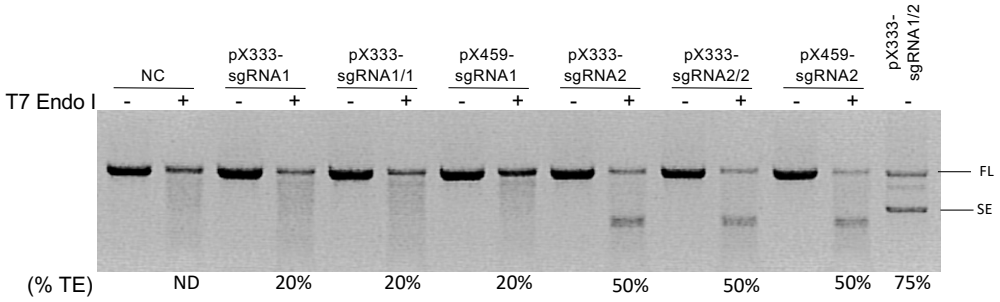

B

sgRNA1

Deletions **Lenght**

```
GTGGAGGAACAGCACAGGCCTTAGTGGGATACTCAGAACGTCATGGCCAGGTGGGATGTGGGATGACAG (X8)
-------------------------TGGGATACTCAGAACGTCATGGCCAGGTGGGATGTGGGATGACAG      -267bp
```

Insertion

```
GTGGAGGAACAGCACAGGCCTTAG-TGGGATACTCAGAACGTCATGGCCAGGTGGGATGTGGGATGACA
GTGGAGGAACAGCACAGGCCTTAGTTGGGATACTCAGAACGTCATGGCCAGGTGGGATGTGGGATGACA      +1bp
```

Editing Efficency 20%

sgRNA1-1

Deletions

```
GTGGAGGAACAGCACAGGCCTTAGTGGGATACTCAGAACGTCATGGCCAGGTGGGATGTGGGATGACAG (X8)
---------------------------GGATACTCAGAACGTCATGGCCAGGTGGGATGTGGGATGACAG      -930bp
---------------------------------------------GCCAGGTGGGATGTGGGATGACAG      -209bp
```

Editing Efficency 20%

sgRNA2

Deletions **Lenght**

```
CCAGACAGGCAGCCAGCTGTTCCTCCTTTAAGGGTGACTCCCTCGATGTTAACCATTCTCCTTCTCCCC (x3)
CC----------------------------AAGGGTGACTCCCTCGATGTTAACCATTCTCCTTCTCCCC  -27bp
CCAGACAGGCAGCCAGCT------------------------------------------------------ (X2) -378bp
```

Insertion

```
CCAGACAGGCAGCCAGCTGTTCCTCCTTT-AAGGGTGACTCCCTCGATGTTAACCATTCTCCTTCTCCC
CCAGACAGGCAGCCAGCTGTTCCTCCTTTTAAGGGTGACTCCCTCGATGTTAACCATTCTCCTTCTCCC  +1bp
```

Editing Efficency **50%**

sgRNA2-2

Deletions

```
CCAGACAGGCAGCCAGCTGTTCCTCCTTTAAGGGTGACTCCCTCGATGTTAACCATTCTCCTTCTCCCC (X5)
CCAGACAGGCAGCCAGCTGTTCCTCCTT-------------------------------------------  -181bp
CCAGACAGGCAGCCAGCTGTCC--------------------CTCGATGTTAACCATTCTCCTTCTCCCC (X2) -19bp
CCAGACAGGCAGCCAGCTGTTC------TTAAGGGTGACTCCCTCGATGTTAACCATTCTCCTTCTCCCC  -5bp
```

Insertion

```
CCAGACAGGCAGCCAGCTGTTCCTCCTTTAA-----GG------TGACTCCCTCGATGTTAACCATTCTC
CCAGACAGGCAGCCAGCTGTTCCTCCTTTAACAGCAGGAACAGTGACTCCCTCGATGTTAACCATTCTC  +10bp
```

Editing Efficency **50%**

sgRNA1–2

Lenght

```
CCAGACAGGCAGCCAGCTGTTCCTCCTTTAAGGGTG(446bp)GAACAGCACAGGCCTTAGTGGGATACTCAGAACGT (X3)
CCAGACAGGCAGCCAG---------------------(446bp)--------------------GGATACTCAGAACGT  -486bp
CCAGACAGGCAGCCAGCTGTTCCTC------------(446bp)----------------------GATACTCAGAACGT  -478 bp
CCAGACAGGCAGCCAGCTGTTCCTCT-----------(446bp)------------------TGGGATACTCAGAACGT (X2) -474 bp
CCAGACAGGC---------------------------(446bp)------------------TGGGATACTCAGAACGT  -490bp
CCAGACAGGCAGCCAGCTGTTCCTCTT----------(446bp)----------------------ATACTCAGAACGT  -477 bp
CCAGACAGGCAGCCAGCTGTTCCTCT-----------(446bp)------------------TGGGATACTCAGAACGT  -474 bp
CCAGACAGGC---------------------------(446bp)------------------------ACTCAGAACGT (X2) -497 bp
```

Editing Efficency 75%

Fig.2

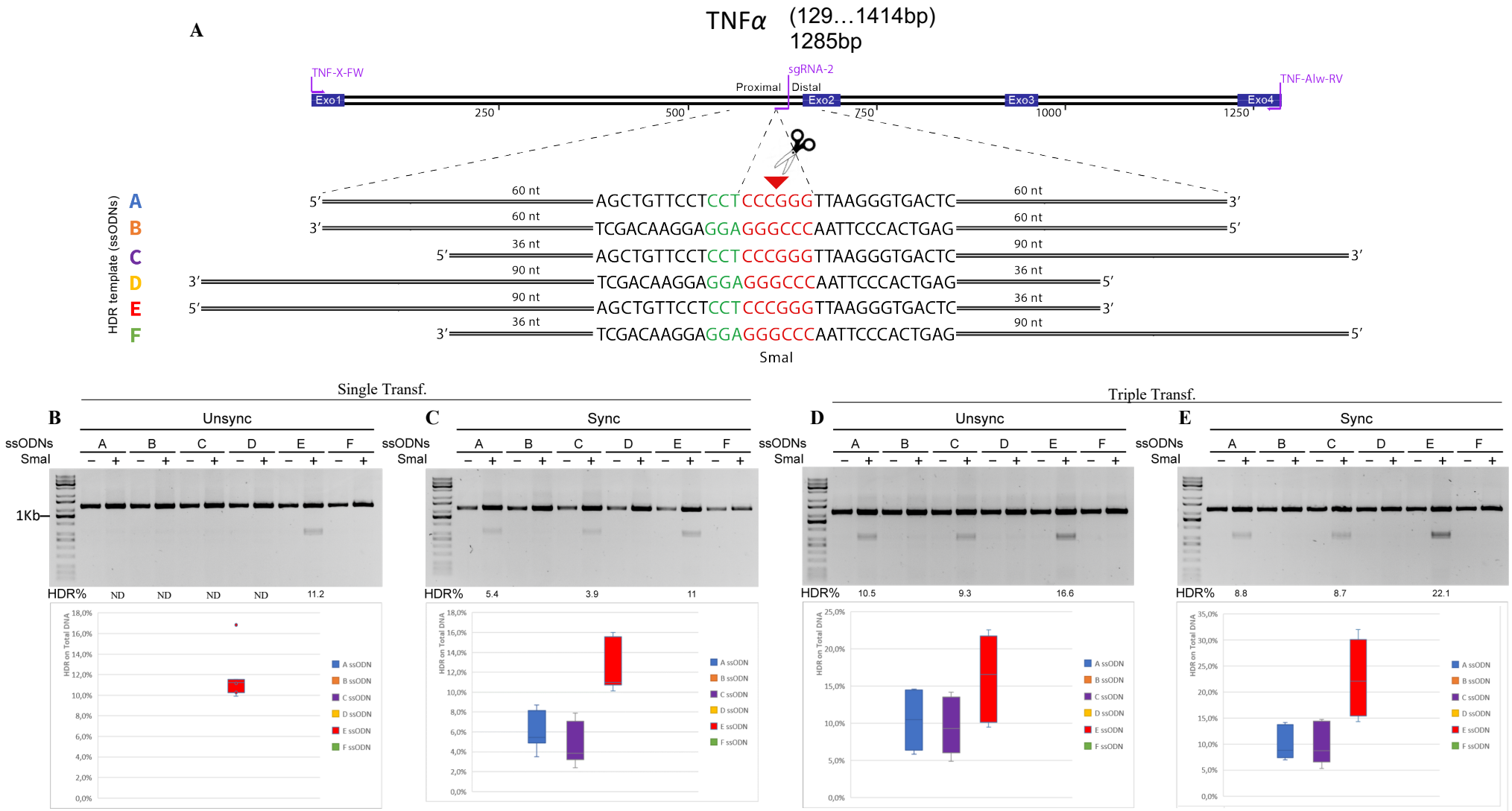
A
TNFα (129…1414bp)
1285bp
TNF-X-FW
sgRNA-2
TNF-AIw-RV
Proximal
Distal
Exo1
Exo2
Exo3
Exo4
250
500
750
1000
1250
HDR template (ssODNs)
A 5′ 60 nt AGCTGTTCCTCCTCCCGGGTTAAGGGTGACTC 60 nt 3′
B 3′ 60 nt TCGACAAGGAGGAGGGCCCAATTCCCACTGAG 60 nt 5′
C 5′ 36 nt AGCTGTTCCTCCTCCCGGGTTAAGGGTGACTC 90 nt 3′
D 3′ 90 nt TCGACAAGGAGGAGGGCCCAATTCCCACTGAG 36 nt 5′
E 5′ 90 nt AGCTGTTCCTCCTCCCGGGTTAAGGGTGACTC 36 nt 3′
F 3′ 36 nt TCGACAAGGAGGAGGGCCCAATTCCCACTGAG 90 nt 5′
SmaI
Single Transf.
Triple Transf.
B Unsync
C Sync
D Unsync
E Sync
ssODNs A B C D E F
SmaI − + − + − + − + − + − +
1Kb
HDR% ND ND ND ND 11.2
HDR% 5.4 3.9 11
HDR% 10.5 9.3 16.6
HDR% 8.8 8.7 22.1
HDR on Total DNA
A ssODN
B ssODN
C ssODN
D ssODN
E ssODN
F ssODN

Fig.3

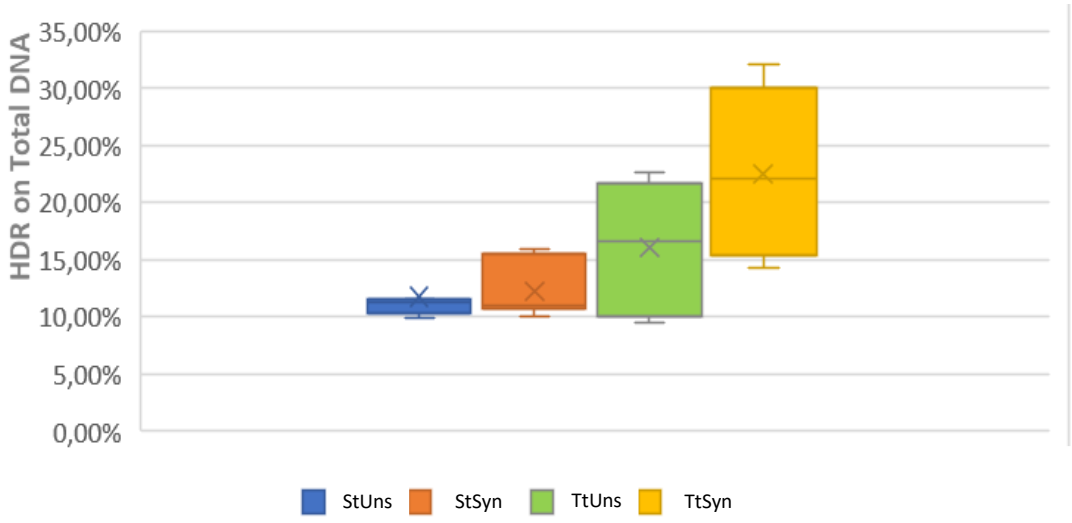
HDR on Total DNA
35,00%
30,00%
25,00%
20,00%
15,00%
10,00%
5,00%
0,00%
StUns
StSyn
TtUns
TtSyn

Fig.4

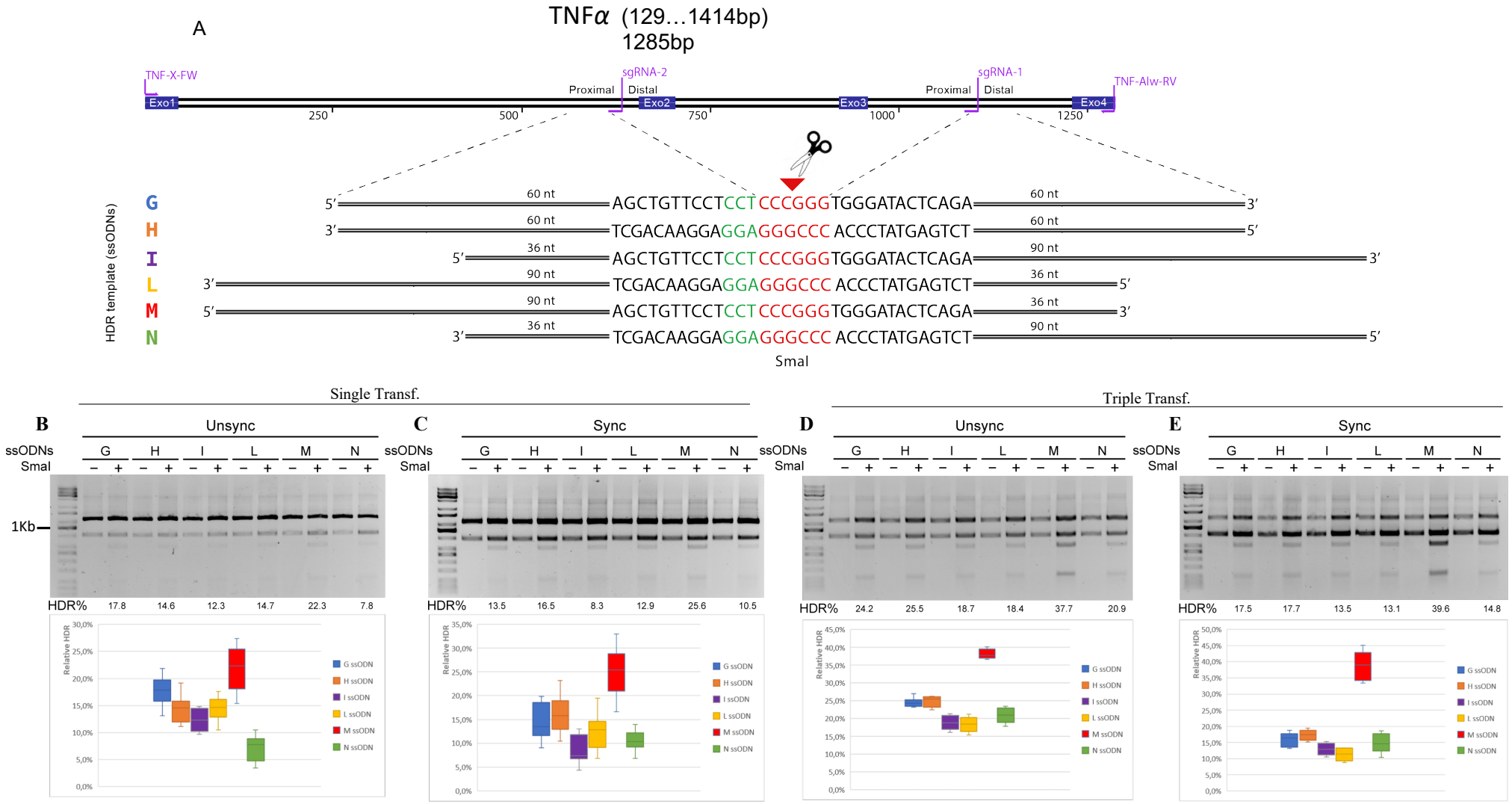
A
TNFα (129…1414bp)
1285bp
TNF-X-FW
sgRNA-2
Proximal
Distal
sgRNA-1
Proximal
Distal
TNF-Alw-RV
Exo1
Exo2
Exo3
Exo4
250
500
750
1000
1250
HDR template (ssODNs)
G
H
I
L
M
N
60 nt
36 nt
90 nt
AGCTGTTCCTCCTCCCGGGTGGGATACTCAGA
TCGACAAGGAGGAGGGCCCACCCTATGAGTCT
SmaI
Single Transf.
Triple Transf.
B
C
D
E
Unsync
Sync
ssODNs
SmaI
1Kb
HDR%
17.8 14.6 12.3 14.7 22.3 7.8
13.5 16.5 8.3 12.9 25.6 10.5
24.2 25.5 18.7 18.4 37.7 20.9
17.5 17.7 13.5 13.1 39.6 14.8
Relative HDR
G ssODN
H ssODN
I ssODN
L ssODN
M ssODN
N ssODN

Fig.5

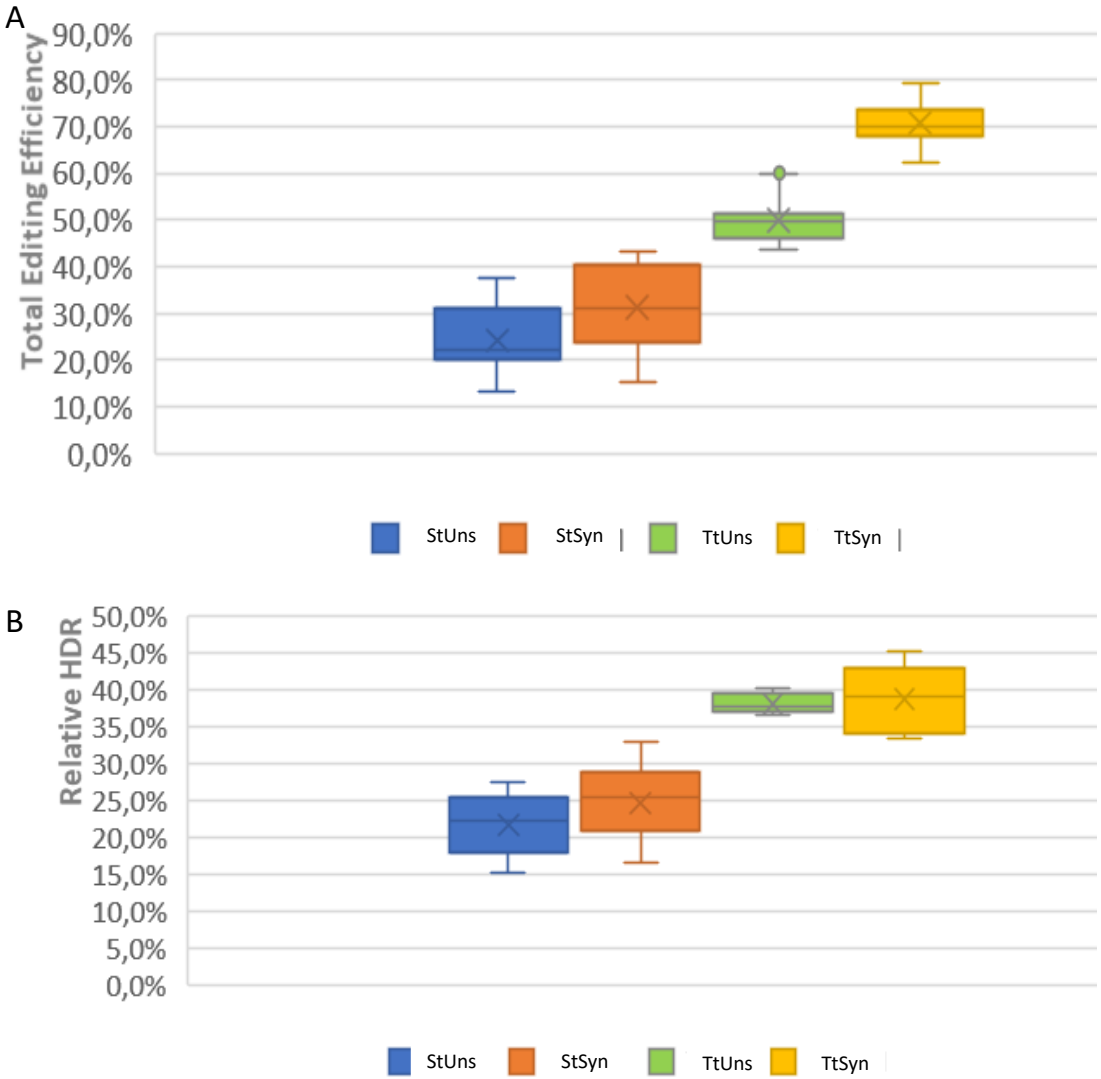
A
Total Editing Efficiency
90,0%
80,0%
70,0%
60,0%
50,0%
40,0%
30,0%
20,0%
10,0%
0,0%
StUns
StSyn
TtUns
TtSyn
B
Relative HDR
50,0%
45,0%
40,0%
35,0%
30,0%
25,0%
20,0%
15,0%
10,0%
5,0%
0,0%
StUns
StSyn
TtUns
TtSyn

Fig.6

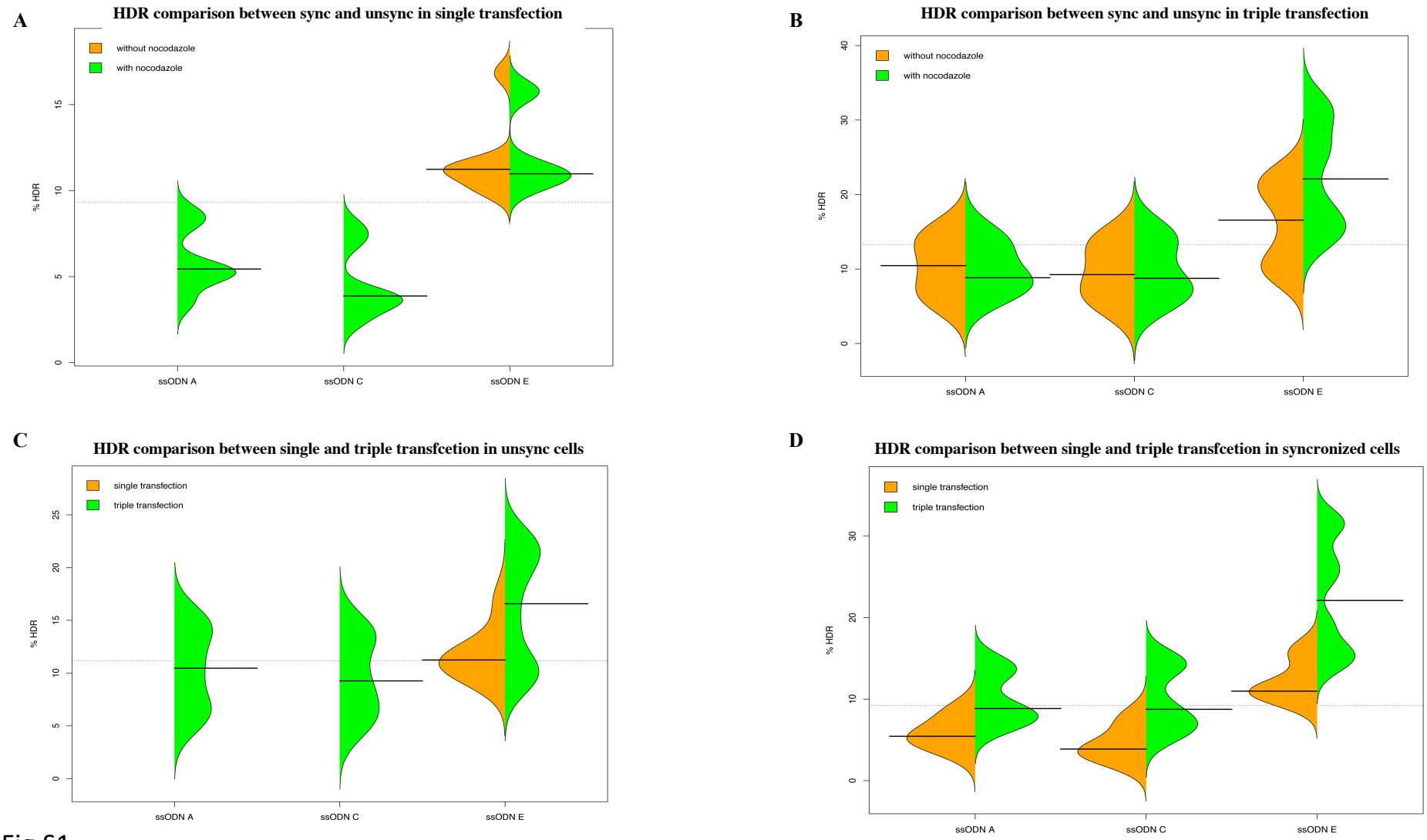
A
HDR comparison between sync and unsync in single transfection
without nocodazole
with nocodazole
% HDR
0
5
10
15
ssODN A
ssODN C
ssODN E
B
HDR comparison between sync and unsync in triple transfection
without nocodazole
with nocodazole
% HDR
0
10
20
30
40
ssODN A
ssODN C
ssODN E
C
HDR comparison between single and triple transfcetion in unsync cells
single transfection
triple transfection
% HDR
0
5
10
15
20
25
ssODN A
ssODN C
ssODN E
D
HDR comparison between single and triple transfcetion in syncronized cells
single transfection
triple transfection
% HDR
0
10
20
30
ssODN A
ssODN C
ssODN E

Fig.S1

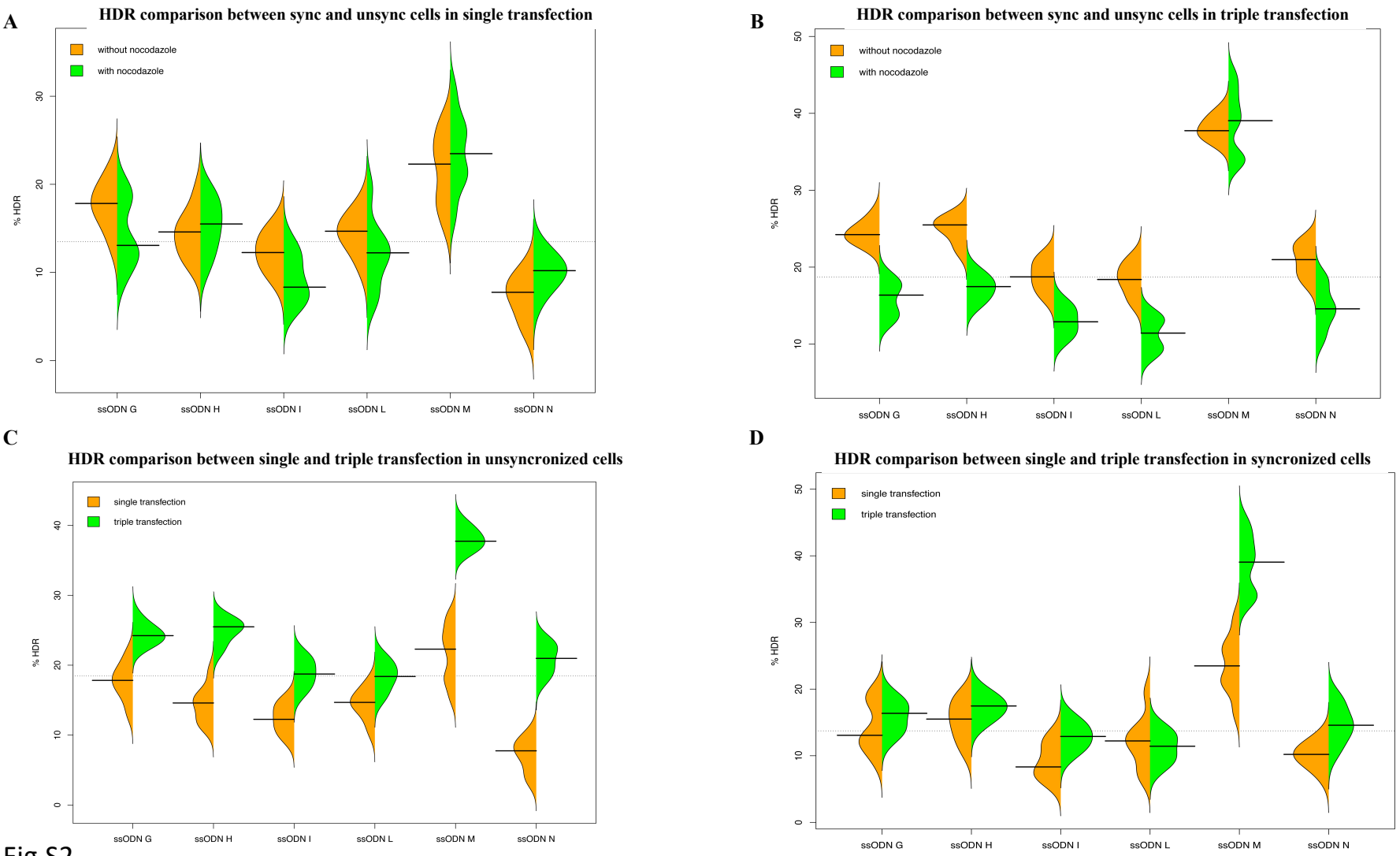
A
HDR comparison between sync and unsync cells in single transfection
without nocodazole
with nocodazole
% HDR
0
10
20
30
ssODN G
ssODN H
ssODN I
ssODN L
ssODN M
ssODN N
B
HDR comparison between sync and unsync cells in triple transfection
without nocodazole
with nocodazole
% HDR
10
20
30
40
50
ssODN G
ssODN H
ssODN I
ssODN L
ssODN M
ssODN N
C
HDR comparison between single and triple transfection in unsyncronized cells
single transfection
triple transfection
% HDR
0
10
20
30
40
ssODN G
ssODN H
ssODN I
ssODN L
ssODN M
ssODN N
D
HDR comparison between single and triple transfection in syncronized cells
single transfection
triple transfection
% HDR
0
10
20
30
40
50
ssODN G
ssODN H
ssODN I
ssODN L
ssODN M
ssODN N

Fig.S2

A

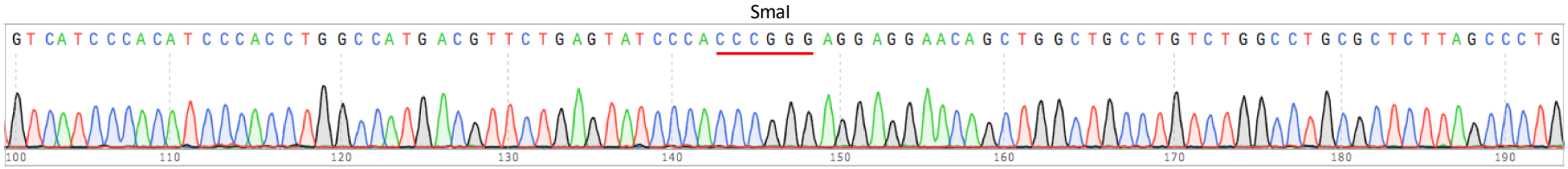
SmaI
GTCATCCCACATCCCACCTGGCCATGACGTTCTGAGTATCCCACCCGGGAGGAGGAACAGCTGGCTGCCTGTCTGGCCTGCGCTCTTAGCCCTG
100
110
120
130
140
150
160
170
180
190

B

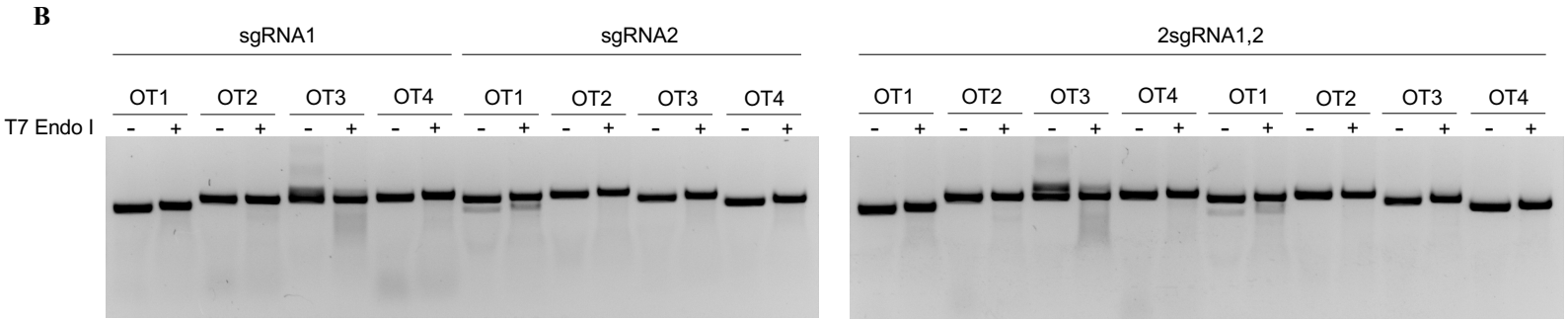
sgRNA1
sgRNA2
2sgRNA1,2
OT1
OT2
OT3
OT4
T7 Endo I
- +

Fig.S3